



**Decoding long-term trends in the wet deposition of sulfate, nitrate
and ammonium after reducing the perturbation from climate
anomalies**

Xiaohong Yao¹, Leiming Zhang²

¹Key Lab of Marine Environmental Science and Ecology, Ocean University of China,
Qingdao 266100, China

²Air Quality Research Division, Science and Technology Branch, Environment and
Climate Change Canada, Toronto, Canada

Correspondence to: X. Yao (xhyao@ouc.edu.cn) and L. Zhang (leiming.zhang@canada.ca)



1 **Abstract.** Long-term trends of wet deposition of inorganic ions are affected by
2 multiple factors, among which emission changes and climate conditions are dominant
3 ones. To assess the effectiveness of emission reductions on the wet deposition of
4 pollutants of interest, contributions from these factors to the long-term trends of wet
5 deposition must be isolated. For this purpose, a two-step approach for preprocessing
6 wet deposition data is presented herein. This new approach aims to reduce the impact
7 of climate anomalies on the trend analysis so that the impact of emission reductions on
8 the wet deposition can be revealed. This approach is applied to a two-decade wet
9 deposition dataset of sulfate (SO_4^{2-}), nitrate (NO_3^-) and ammonium (NH_4^+) at rural
10 Canadian sites. Analysis results show that the approach allows for robustly identifying
11 inflection points on decreasing trends in the wet deposition fluxes of SO_4^{2-} and NO_3^- in
12 northern Ontario and Québec. The inflection points match well with the three-phase
13 mitigation of SO_2 emissions and two-phase mitigation of NO_x emissions in Ontario.
14 Improved correlations between the wet deposition of ions and their precursors'
15 emissions were obtained after reducing the impact from climate anomalies.
16 Furthermore, decadal climate anomalies were identified as dominating the decreasing
17 trends in the wet deposition fluxes of SO_4^{2-} and NO_3^- at a western coastal site. Long-
18 term variations in NH_4^+ wet deposition showed no clear trends due to the compensating
19 effects between NH_3 emissions, climate anomalies, and chemistry associated with the
20 emission changes of sulfur and nitrogen.

21

22 **1. Introduction**

23 To assess the long-term impacts of acidifying pollutants on the environment, the wet
24 deposition of sulfate (SO_4^{2-}), nitrate (NO_3^-) and ammonium (NH_4^+), among other
25 inorganic ions, has been measured for several decades through monitoring networks



26 such as the European Monitoring and Evaluation Programme (EMEP) (Fowler et al.,
27 2005, 2007; Rogora et al., 2004, 2016), the National Atmospheric Deposition
28 Program/National Trends Network in the U.S. (Baumgardner et al., 2002; Lehmann et
29 al., 2007; Sickles & Shadwick, 2015), and the Canadian Air and Precipitation
30 Monitoring Network (CAPMoN) (Vet et al., 2014; Zbieranowski and Aherne, 2011).
31 The high-quality data collected from these networks have been widely used to quantify
32 the atmospheric deposition of acidifying pollutants (Lajtha & Jones, 2013; Lynch et al.,
33 2000; Pihl Karlsson et al., 2011; Strock et al., 2014; Vet et al., 2014). The data have
34 also been utilized to identify trends in the atmospheric deposition of reactive nitrogen
35 (Fagerli & Aas, 2008; Fowler et al., 2007; Lehmann et al., 2007; Zbieranowski and
36 Aherne, 2011) and to examine the impacts of acid rain and the perturbation of the
37 natural nitrogen cycle on sensitive ecosystems (Wright et al., 2018). The long-term data
38 can also be used for assessing the effectiveness of environmental policies (Butler et al.,
39 2005; Li et al., 2016; Lloret & Valiela, 2016).

40

41 The wet deposition of SO_4^{2-} , NO_3^- and NH_4^+ is affected by not only their gaseous
42 precursors' emissions (Butler et al., 2005; Fowler et al., 2007; Li et al., 2016) but also
43 complex atmospheric processes (Cheng & Zhang, 2017; Yao & Zhang, 2012; Zhang et
44 al., 2012). Those atmospheric processes sometimes lead to extremely high wet
45 deposition fluxes of ions during a precipitation event or even throughout a particular
46 month. Furthermore, climate anomalies can alter the relative contributions of local
47 sources versus long-range transport to the total wet deposition amounts at reception
48 sites, thereby complicating the relationships between wet deposition and the emission
49 of air pollutants of interest (Lloret & Valiela, 2016; Monteith et al., 2016; Wetherbee
50 & Mast, 2016). The emissions of SO_2 and NO_x have been decreasing substantially in



51 Europe and North America (Butler et al., 2005; Li et al., 2016; Pihl Karlsson et al.,
52 2011); coincidentally, climate anomalies have also occurred more frequently in recent
53 decades (Burakowski et al., 2008; Lloret & Valiela, 2016; Wijngaard et al., 2003),
54 thereby leading to more complicated linkages between wet deposition and emission
55 trends on decadal scales.

56

57 Many trend analysis studies in the literature simply examined annual or seasonal values
58 as the data inputs for two popular trend analysis tools, i.e., the Mann-Kendall (M-K)
59 and linear regression (LR) methods (Marchetto et al., 2013; Waldner et al., 2014 and
60 references therein). These studies focused on the detection of statistically significant
61 trends; for example, Waldner et al. (2014) conducted a comprehensive analysis on the
62 applicability of the techniques to different choices of length and temporal resolutions
63 of a data series. Regarding the resolved trend results, these approaches are not well
64 suited to separating the impact of air pollutants' mitigation from the perturbation by
65 climate anomalies. Large uncertainties thus existed in the studies interpreting the major
66 driving forces determining the extracted trends in the wet deposition of SO_4^{2-} , NO_3^- and
67 NH_4^+ . Regarding that air pollutant's emission mitigation targets often vary in different
68 phases of the entire study period, inflection points may exist in the trends in the wet
69 deposition of ions. The inflection points were rarely studied, despite their importance
70 for assessing the effectiveness of environmental policies. An alternative would be to
71 use high time resolution data in the Ensemble Empirical Mode Decomposition (EEMD)
72 method (Wu & Huang, 2009); however, this method still suffers from the end effect in
73 certain scenarios, whereby the extracted trends cannot be explained (Yao & Zhang,
74 2016).

75



76 A new approach is presented herein that aims to reduce the perturbations from climate
77 anomalies on data inputs so that robust trends can be elucidated for evaluating the
78 effectiveness of emission control policies. In this approach, raw data are preprocessed
79 to generate a new variable, which is then applied to M-K and LR methods. A piecewise
80 linear regression (PLR) is also used to extract trends for cases in presence of inflection
81 points. The extracted trends in the wet deposition data on a decadal scale are then
82 properly linked to major driving forces such as emission reductions and climate
83 anomalies. This new approach is first applied to the wet deposition data of SO_4^{2-} , NO_3^-
84 and NH_4^+ in Canada, as an example to demonstrate its capability and advantages over
85 the traditional approaches. The extracted trends in the wet deposition of ions are further
86 studied through correlation analysis with known emission trends of their respective
87 gaseous precursors (SO_2 , NO_x and NH_3) in Canada and the U.S. Major driving forces
88 for the trends of ion wet deposition and how the wet deposition ions responded to their
89 precursors' emissions in Canada are then revealed.

90

91 **2. Methodology**

92 Wet deposition flux (F_{wet}) data were obtained from CAPMoN
93 ([https://www.canada.ca/en/environment-climate-change/services/air-](https://www.canada.ca/en/environment-climate-change/services/air-pollution/monitoring-networks-data/canadian-air-precipitation.html)
94 [pollution/monitoring-networks-data/canadian-air-precipitation.html](https://www.canada.ca/en/environment-climate-change/services/air-pollution/monitoring-networks-data/canadian-air-precipitation.html)). Data from four
95 sites have been collected for over twenty years and were chosen herein to illustrate the
96 novel trend analysis method (Table S1). Site 1 is an inland forest site at Chapais in
97 Québec. Site 2 is situated in a coastal forest area at Saturna in British Columbia. Sites
98 3 and 4 are two inland forest sites at the Chalk River and at Algoma, respectively, in
99 northern Ontario. Details on data sampling, chemical analysis and quality control can
100 be found in previous studies (Cheng & Zhang, 2017; Vet & Ro, 2008; Vet et al., 2014).



101 The emissions data of gaseous precursors were downloaded from the Air Pollutant
102 Emission Inventory (APEI, <https://pollution-waste.canada.ca/air-emission-inventory/>)
103 in Canada and from the USEPA National Emissions Inventory (NEI,
104 <https://www.epa.gov/air-emissions-inventories/air-emissions-sources>) in the U.S.
105 These data were demarcated at a provincial level in Canada and at a state level in the
106 U.S. Data for the years of 1990 to 2011, which correspond to the period of selected F_{wet}
107 data, were used in this study.

108

109 The M-K method is a popular nonparametric statistical procedure that can yield
110 qualitative trend results, such as “an increasing/decreasing trend with a P value of
111 <0.05 ,” “a probable increasing/decreasing trend with a P value of $0.05-0.1$,” “a stable
112 trend with a P value of >0.1 , as well as a ratio of <1.0 between the standard deviation
113 and the mean of the dataset,” and “a no trend for $P>0.1$ with all other conditions”
114 (Kampata et al., 2008; Marchetto et al., 2013). The LR method has also been widely
115 used to extract trends (Marchetto et al., 2013; Waldner et al., 2014). Zbieranowski and
116 Aherne (2011) used LR to extract trends by separating different phases because of the
117 presence of inflection points in the entire study period, and the approach is same as PLR
118 (Vieth, 1989). In this study, the three methods were employed to compute the trends
119 of ion wet deposition using software downloaded from [https://www.gsi-](https://www.gsi-net.com/en/software/free-software/gsi-mann-kendall-toolkit.html)
120 [net.com/en/software/free-software/gsi-mann-kendall-toolkit.html](https://www.gsi-net.com/en/software/free-software/gsi-mann-kendall-toolkit.html) and Excel 2016, first
121 using the annual F_{wet} directly as input data, then using a modified input data set, as
122 described below.

123

124 The modified input data set was produced in two steps. The first step was an effort to
125 reduce the perturbation from the monthly climate anomalies to the input data. This was



126 done by creating a new variable that was defined as the slopes of the regression
127 equations of a series of study years against a climatology (base) year using monthly
128 F_{wet} data. Note that the monthly F_{wet} data were aggregated from daily raw data before
129 the regression analysis. To ensure the presence of enough data points in each regression
130 equation, the data corresponding to two-year periods (or 24 monthly F_{wet} values) were
131 grouped together, as detailed below. At a selected site and for a given chemical
132 component, monthly F_{wet} data were generated for the first two years and were grouped
133 together and rearranged from the smallest to the largest values to form an array of data
134 with 24 data points, i.e., $A(i)$ with $i=1$ to 24. Repeating the above procedure for the
135 subsequent years using a two-year interval to eventually obtain a series of data arrays,
136 $A(i)$ now becomes $A(i, j)$ with $i=1$ to 24 and $j=1$ to N , where N is the total number of
137 data arrays. The climatology data array ($CA(i)$) was then defined as the average of all
138 of the arrays as follows:

$$139 \quad CA(i) = \frac{1}{N} \sum_{j=1}^N A(i, j), \quad i = 1 \text{ to } 24.$$

140

141 LR with zero interception was applied for each individual data array against the
142 climatology data array. In cases where the maximum monthly deposition flux deviated
143 greatly from the general regression curve, the slopes (m -values) were calculated after
144 excluding the maximum monthly deposition flux, which is an approach that reduced
145 the perturbation to the m -values from the monthly scale climate anomalies. The second
146 step was to screen out the outliers in m -values, which reduced the perturbation to the
147 m -values from the annual-scale climate anomalies.

148

149 An analysis of Site 1 is used to illustrate the new approach and demonstrate its
150 advantages against the existing common approaches used in the literature. Twelve four-



151 year periods of data (1988-1989, 1990-1991, etc.) are available from this site. The
152 regression of each data set against the climatology data set was first performed using
153 all of the monthly values to obtain an m-value (the slope) (Fig. 1a-d). For eight out of
154 the 12 data sets, the m-values were recalculated after excluding the maximum monthly
155 value of F_{wet} , which appeared to be an apparent outlier of the linear regression. The R^2
156 values, which are conventionally used in LR, were then significantly increased for these
157 eight sets, e.g., from the original values of 0.79-0.94 to the improved values of 0.92-
158 0.98. To demonstrate that the excluded maximum value was an outlier, the case of the
159 1990-1991 data set was taken as an example. The new regression equation ($y=1.47x$,
160 $R^2=0.98$, Fig. 1a) predicted a maximum value in the range of 330-368 $\text{mg m}^{-2} \text{month}^{-1}$
161 using three times the standard deviation ($\pm 3 \text{ SD}$, 0.08) at a 99% confidence level. The
162 actual observed maximum value of 532 $\text{mg m}^{-2} \text{month}^{-1}$ was much larger than the upper
163 range of the predicted value and was thus believed to be caused by monthly scale
164 climate anomalies. The maximum value was treated as an outlier and excluded for
165 analysis. Using the similar procedure, all outliers in this study were identified. The
166 exclusion of the observed maximum value greatly reduced the perturbation of the short-
167 term climate anomalies to the calculated m-value in this two-year period, i.e., the m-
168 value decreased from 1.67 to 1.47, which in turn increased the relative contribution of
169 the air pollutants' emissions to the calculated m-value. In summary, this new approach
170 meets the objective of identifying outlier data points by applying the criteria of being
171 outside the boundaries of ± 3 times the standard deviation of the general trend.

172

173 The revised m-values were further scrutinized by eliminating the outliers caused by the
174 annual-scale climate anomalies. For example, the m-value of 1.31 in 1998-1999 greatly
175 deviated from other m-values, narrowly oscillating approximately 0.96 ± 0.07 (average



176 ± 1 SD) during the period of 1994-2005, even with the ± 3 SD being considered (Fig.
177 1a-d). Using the value of 0.96 as the reference, climate anomalies likely increased the
178 F_{wet} of SO_4^{2-} by 37% in 1998-1999. The m-values were then calculated by shifting one
179 year in time to 1997-1998 (1.07) and to 1999-2000 (1.24). The F_{wet} in 1998 was less
180 affected by climate anomalies than that in 1999. Thus, the m-value in 1997-1998 was
181 within 0.96 ± 0.21 (average ± 3 SD) and used to replace the m-value in 1998-1999 for
182 the trend analysis. Similar to the first step discussed above, this approach meets the
183 objective of identifying outlier m-values by applying the criteria of being outside the
184 range of ± 3 SD plus the average m-value during a decade or a longer period.

185

186 More justification of the new approach can be found in the Supporting Information,
187 including Figs. S1-3, wherein the statistical comparison between this and other
188 approaches was presented. Theoretically, the extracted trend using the data
189 preprocessed with the new approach is determined by the local emissions of air
190 pollutants, the regional transport of air pollutants, and a small portion of climate
191 anomalies that are unable to be removed by the new approach. It is assumed that the
192 extracted trend is less affected by microphysical/chemical processes, since two-year
193 data were used together to calculate the m-value.

194

195 In theory, if the data from different sites in the same region are grouped together for
196 trend analysis, the results may be better linked to the trends of the regional emissions
197 of related air pollutants. In the following sections, trend analysis results from individual
198 sites as well as those from grouped sites are discussed. Sites 1, 3 and 4 showed similar
199 trends in the wet deposition of SO_4^{2-} and NO_3^- , and these three sites were grouped
200 together.



201 **3. Results and discussion**

202 *3.1 Trends at Site 1 after reducing perturbations from climate anomalies*

203 Trends in the m-values shown in Fig. 2 represent the trends after removing the
204 perturbations from climate anomalies at Site 1 in northern Québec from 1988 to 2011.
205 SO_4^{2-} and NO_3^- showed decreasing trends from a LR analysis, with R^2 values of 0.81
206 and 0.71, respectively, and P values <0.01 . The decreasing trends were also confirmed
207 by the M-K method analysis. NH_4^+ exhibited a stable trend from M-K analysis, as well
208 as no significant trend with P value >0.05 from LR analysis.

209

210 The m-values of SO_4^{2-} and NO_3^- also allowed for the identification of trends in different
211 phases. The inflection point for each phase is critical to a) link the annual F_{wet} of ions
212 and the emissions of the corresponding precursors and b) assess the effectiveness of
213 environmental policies. For example, the trends in the m-values of SO_4^{2-} can be clearly
214 classified into three phases. The m-values oscillated approximately 1.38 ± 0.08 during
215 Phase 1 (1988 to 1993) and approximately 1.02 ± 0.08 during Phase 2 (1994 to 2005),
216 with a significant difference between the two phases under the t-test (P value <0.01),
217 thereby implying an abrupt decrease of approximately 30% at the inflection point
218 between the two phases. In contrast, the m-values linearly decreased by approximately
219 20% every two years, starting from the end of Phase 2 to Phase 3 (2006-2011). Again,
220 a significant difference existed between Phase 2 and Phase 3 under the t-test (P value
221 <0.01). Overall, PLR should be applied separately for the different phases in the
222 presence of the inflection points, rather than LR for the entire period, and the result is
223 presented as:

224

$$\begin{cases} m - \text{value} = 1.38, 1988 \leq x < 1994 \\ m - \text{value} = 1.02, 1994 \leq x \leq 2004 \\ m - \text{value} = -0.185 * \left(\frac{x}{2} - 1001\right) + 1.15, 2004 < x \leq 2010 \end{cases}$$



225 where x represent the calendar year from 1988 to 2010.

226

227 The trend in the m -values of NO_3^- can be classified into two phases, with the inflection
228 point at 2003, according to the t -test result, i.e., the values oscillated approximately
229 1.09 ± 0.09 during the period from 1988 to 2003 and then exhibited a significant decrease
230 of approximately 50% overall afterwards, with P value < 0.01 . The PRL result is
231 expressed as below:

$$232 \quad \begin{cases} m - \text{value} = 1.09, 1988 \leq x < 2004 \\ m - \text{vlaue} = -0.128 * \left(\frac{x}{2} - 1001\right) + 1.08, 2004 \leq x \leq 2010 \end{cases}$$

233 The m -value of NO_3^- in 1998-1999 was approximately 30% larger than the mean value
234 in 1988-2003 and exceeded the mean value plus 3 SD in 1998-2003, and thus was not
235 included in the trend analysis. The sharp increase in F_{wet} of NO_3^- occurred mainly in
236 1999, which was probably caused by a large perturbation from climate anomalies.
237 Moreover, the monthly F_{wet} values of NO_3^- in March, April, July and August 1999 were
238 actually lower than the corresponding long-term averages in 1988-2003 (excluding
239 1999) (Fig. S4a). This outcome indicates that the large increase in annual F_{wet} of NO_3^-
240 in 1999 was unlikely to have been determined by the emissions of its gaseous
241 precursors. The same can be said for the large increase in F_{wet} of SO_4^{2-} in 1999 (Fig. 2a,
242 S4b).

243

244 The trends in the m -value of SO_4^{2-} at Site 1 (Fig. 2a) were clearly different from those
245 of the SO_2 emissions in Québec (Fig. 2c) but matched well to those in Ontario (Fig. 2c),
246 which is also supported by their Pearson correlation coefficients, e.g., no significant
247 correlation ($r = 0.46$ and P value > 0.05) for the former case and a good correlation ($r =$
248 0.96 and P value < 0.01) for the latter case. Note that r instead of R^2 is conventionally



249 used in correlation analysis and is therefore used here. Zhang et al. (2008) reported that
250 this remote area can receive the long-range transport of air pollutants from Ontario but
251 that transport is less likely from the intensive emission sources in Québec.

252

253 The trends in NO_x emissions during 1990-2003 had similar bell-shape patterns in
254 Québec and Ontario, although with different magnitudes of emissions (Fig. 2f). A
255 different trend pattern was seen for the m-value of NO₃⁻ at Site 1 than for the
256 abovementioned provincial emissions during the same period (Fig. 2d), and there was
257 no significant correlation ($r < 0.41$, with P value > 0.05) between the m-value of NO₃⁻
258 and the emissions of NO_x in Québec or Ontario. Different results were found for the
259 period of 2002-2011 than those of 1990-2003 discussed above. In 2002-2011, the m-
260 value of NO₃⁻ decreased by ~50% and the NO_x emissions decreased by ~40% in
261 Québec and Ontario; also, good correlations ($r = 0.94-0.95$ with P values < 0.01) were
262 observed between m-values and emissions. The contrasting results between the two
263 different periods discussed above implied one possibility, i.e., that the perturbation
264 from climate anomalies, which was unable to be removed by the new approach,
265 overwhelmed the effect of NO_x emissions on trends in m-values of NO₃⁻ in 1990-2003,
266 while the reverse was true in 2002-2011. However, other possibilities cannot be
267 excluded. F_{wet} of NO₃⁻ and precipitation depth exhibited only a weakly significant
268 correlation, with $r = 0.58$ and $P < 0.05$ in 1988-2003 (the values in 1999 were excluded).
269 Annual precipitation varied by only ~20% during the fifteen years, and this factor alone
270 was unlikely to explain the ~100% interannual variation of F_{wet} of NO₃⁻ during that
271 period.

272

273 The m-values of NH₄⁺ at Site 1 had no significant correlation ($r = 0.21$ and P value



274 >0.05) with the emissions of NH_3 in Québec but exhibited a weakly significant
275 correlation ($r = 0.60$ and P value <0.05) with the emissions of NH_3 in Ontario. Nearly
276 all of the NH_4^+ was associated with SO_4^{2-} and NO_3^- in the atmosphere (Cheng and
277 Zhang, 2017; Teng et al., 2017; Tost et al., 2007; Zhang et al., 2012), and the trends in
278 the m -value of NH_4^+ could be affected by many other factors besides NH_3 emissions
279 and climate anomalies.

280

281 LR analysis of the annual F_{wet} of these ions revealed decreasing trends for SO_4^{2-} and
282 NO_3^- (second row in Fig. 2). The M-K method analysis also confirmed the decreasing
283 trends with annual F_{wet} as input. However, the three-phase trends in F_{wet} of SO_4^{2-} and
284 the two-phase trends in F_{wet} of NO_3^- and related inflection points, identified using the
285 m -values discussed above, were not identified by the t -test when simply using annual
286 F_{wet} data as input. The correlations between annual F_{wet} and emissions were 0.89 for
287 SO_4^{2-} vs. SO_2 in Ontario and 0.74-0.76 for NO_3^- vs. NO_x in Québec and Ontario (P
288 values <0.01), while the corresponding r values were as high as 0.95 and 0.84-0.85
289 between m -values and emissions. After reducing the perturbations from climatic factors
290 to the annual F_{wet} , stronger correlations were obtained between F_{wet} and emissions.

291

292 The stable trend in annual F_{wet} of NH_4^+ and the decreasing trend in annual F_{wet} of NO_3^-
293 gradually increased the relative contributions of reduced nitrogen in the total nitrogen
294 wet deposition budget, e.g., from 40% in 1998-1999 to 52% in 2010-2011. A similar
295 trend has also been recently reported in the U.S. (Li et al., 2016). Such a trend was
296 mostly due to the mitigation of NO_x rather than climate anomalies.

297

298 *3.2 Decadal climate anomalies drove trends at Site 2*



299 Fig. 3 shows the trend analysis results at Site 2. An obvious shift in the m-values and
300 annual F_{wet} occurred during 2001-2002, as detected by the t-test, i.e., the m-values of
301 SO_4^{2-} oscillated approximately 1.15 ± 0.11 in 1990-2001 and 0.76 ± 0.02 in 2002-2011
302 (or 0.83 ± 0.12 if the value in 2006-2007 was included), but with a significant difference
303 between the two periods with P value < 0.01 . The annual F_{wet} of SO_4^{2-} oscillated
304 approximately $632 \pm 63 \text{ mg m}^{-2}$ in 1990-2001 and $452 \pm 74 \text{ mg m}^{-2}$ in 2002-2011, and the
305 values between the two periods showed significant differences. The shift led to the m-
306 values and annual F_{wet} of SO_4^{2-} exhibiting a consistent decreasing trend by $\sim 40\%$ overall
307 from 1990 to 2011 using the LR and the M-K method.

308

309 The emissions of SO_2 oscillated approximately 1.13 ± 0.07 in 1990-2001 and 1.06 ± 0.03
310 in 2002-2011 in British Columbia, which did not support the large decrease of
311 approximately 40% in wet deposition of SO_4^{2-} in 2002-2011. Statistically, no
312 correlation existed between annual F_{wet} of SO_4^{2-} and the emissions of SO_2 in British
313 Columbia, with $r = 0.52$ and P value > 0.05 . Although the transboundary transport of air
314 pollutants from the U.S. cannot be excluded, the almost constant m-values from 2002
315 to 2011 (excluding 2006-2007) at Site 2 were inconsistent with the approximately 70%
316 decrease in emissions of SO_2 in the state of Washington in the U.S. during that period
317 (not shown). Precipitation cannot explain the jump in wet deposition either, because
318 there was no corresponding jump in precipitation during 2001-2002 (Fig. 3b).

319

320 van Donkelaar et al. (2008) analyzed aircraft and satellite measurements from the
321 Intercontinental Chemical Transport Experiment and proposed the long-range transport
322 of sulfur from East Asia to the west coast of Canada. The average wind fields in 1990-
323 2011 at different altitudes also showed air masses primarily originating from the Pacific



324 Ocean in the west (Fig. 4a). However, the climate anomalies of wind fields in 1990-
325 2001 compared against 1990-2011 clearly showed a counterclockwise pattern in the
326 corresponding coastal area, including Site 2, while a clockwise pattern existed in 2002-
327 2011 against 1990-2011 (Fig. 4b, c). The decadal climate anomalies of wind fields in
328 2002-2011 very likely caused a large decrease in the contribution of air pollutants from
329 the eastern coast to Site 2, resulting in a distinct demarcation at 2002. This hypothesis
330 was also supported by a large rebound of the m-value in 2006-2007, due to the increase
331 in F_{wet} of SO_4^{2-} in 2007. The climate anomalies of wind fields in 2007 against 1990-
332 2011 showed a counterclockwise pattern in the north, while the clockwise pattern was
333 pushed to the south (Fig. 4d). A greater contribution of air pollutants from the eastern
334 coast to Site 2 might have led to the large increase in F_{wet} of SO_4^{2-} during a few month-
335 long periods in 2007.

336

337 The present study is the first one to identify the decreasing trend in the annual F_{wet} of
338 SO_4^{2-} as being very likely caused by decadal climate anomalies rather than by the
339 emission reductions of SO_2 . The decadal climate anomalies may substantially alter the
340 long-range transport of air pollutants to the reception site. Note that the causes for the
341 decadal climate anomalies in this region are beyond the scope of the present study, but
342 some information can be found in the literature (Bond et al., 2003; Coopersmith et al.,
343 2014; Deng et al., 2014).

344

345 For the wet deposition of NO_3^- , the m-values also showed a clear shift, i.e., the m-values
346 oscillated approximately 1.09 ± 0.14 in 1990-2001 and 0.88 ± 0.06 in 2002-2011, with a
347 significant difference between the two periods under the t-test with P value < 0.01 . The
348 annual F_{wet} of NO_3^- varied substantially, and the shift could not be identified



349 statistically. However, the annual F_{wet} of NO_3^- exhibited a decreasing trend by M-K
350 method analysis. Similar to the case of SO_4^{2-} , no significant correlation ($r = 0.49$, P
351 value >0.05) existed between the annual F_{wet} of NO_3^- and the emissions of NO_x in
352 British Columbia.

353

354 In addition to decadal climate anomalies, the interannual climate variability also
355 affected the trends in m -values and annual F_{wet} of NO_3^- . The perturbations from
356 interannual climate variability cannot be completely removed by the new approach, and
357 they complicate the relationship between the F_{wet} of NO_3^- and the emissions of NO_x in
358 British Columbia. For example, the m -values in 1990-1991, 1996-1997, 1998-1999 and
359 2000-2001 were nearly constant at 1.17 ± 0.03 . However, the NO_x emissions in British
360 Columbia in 1998-1999 were 26% greater than those in 1990-1991. There was a sharp
361 decrease in the NO_x emissions (by $\sim 30\%$) from 2002 to 2011 in British Columbia.
362 However, the m -values oscillated approximately 0.88 ± 0.06 and showed no clear trend
363 based on either the M-K method or LR analysis. The interannual climate variability
364 apparently negated the impact of reduced emissions during these periods.

365

366 The m -values and the annual F_{wet} of NH_4^+ oscillated approximately 0.99 ± 0.13 and
367 $81 \pm 16 \text{ mg m}^{-3}$, respectively, in the period of 1990-2011, and showed no trend (Fig. 3).
368 Neither the m -values nor annual F_{wet} of NH_4^+ showed the two-period distribution
369 pattern or had any significant correlation with the emissions of NH_3 in British Columbia
370 at a 95% confidence level. Similarly to Site 1, the annual variation in F_{wet} of NH_4^+ at
371 Site 2 cannot be simply explained by known emission trends.

372

373 In summary, decadal climate anomalies overwhelmingly determined the long-term



374 trends in the wet deposition of SO_4^{2-} and NO_3^- , with the perturbation from monthly and
375 annual climate anomalies removed at Site 2. The interannual climate variability further
376 complicated the trends, resulting in undetectable influences of the emission trends on
377 the deposition trends. Since the decrease in F_{wet} of NO_3^- appeared to be primarily caused
378 by climate anomalies, the relative contributions of NH_4^+ and NO_3^- in the total N wet
379 deposition varied little, i.e., 33% versus 67% in 2010-2011 and 31% versus 69% in
380 1990-1991.

381

382 *3.3 Regional trends in wet deposition in northern Ontario and Québec*

383 Trends in the m-values or annual F_{wet} of ions at Sites 3 and 4 in the northern regions of
384 Ontario were generally similar to those found at Site 1 (Fig. S5 and S6). For example,
385 the three-phase trend in m-values of SO_4^{2-} and the two-phase trend in m-values of NO_3^-
386 were also obtained at Sites 3 and 4 after excluding a few m-values that were caused by
387 large perturbations from climate anomalies. Thus, Sites 1, 3 and 4 were combined
388 together to study regional trends in the northern areas of Ontario and Québec (Fig. 5a-
389 c). Similar to those found at the individual sites, the temporal profile of regional m-
390 values of SO_4^{2-} can be clearly classified into three phases (Fig. 5a) as follows: Phase 1
391 from 1988 to 1993 with m-values oscillating approximately 1.31 ± 0.08 , Phase 2 from
392 1994 to 2003 with near-constant m-values of 1.05 ± 0.04 , and Phase 3 for 2004 onward
393 with a decreasing trend by an overall $\sim 50\%$. Significant differences of m-values existed
394 between any two of the three phases, based on the t-test results (P value < 0.01). The
395 PRL result is expressed as below:

$$396 \quad \left\{ \begin{array}{l} m - \text{value} = 1.31, 1988 \leq x < 1994 \\ m - \text{value} = 1.05, 1994 \leq x < 2004 \\ m - \text{value} = -0.129 * \left(\frac{x}{2} - 1001\right) + 1.03, 2004 \leq x \leq 2010 \end{array} \right.$$

397 The three-phase pattern of m-values matched well with the three-phase emission profile



398 of SO₂ in Ontario. Statistically, an ~70% decrease in m-value and an ~70% decrease in
399 emissions were found from 1990 to 2011, with a correlation of $r = 0.95$ (P value <0.01).

400

401 The profile of the regional m-values of NO₃⁻ also clearly exhibited two phases,
402 according to the following t-test results between them: Phase 1 from 1988 to 2003, with
403 m-values narrowly varying approximately 1.11 ± 0.05 and Phase 2 from 2004 to 2011,
404 with a decreasing trend by an overall ~40% against that in 2002-2003 (Fig. 5b). The
405 PRL result is expressed as below:

$$406 \quad \begin{cases} m - value = 1.11, 1988 \leq x < 2004 \\ m - value = -0.11 * \left(\frac{x}{2} - 1001\right) + 1.03, 2004 \leq x \leq 2010 \end{cases}$$

407 From 2002 to 2011, the m-value had a moderately good correlation with the NO_x
408 emission in Ontario ($r = 0.91$, $P < 0.01$), and the two variables decreased by 30-40% in
409 this period. From 1990 to 2003, the near constant m-value was, however, inconsistent
410 with the bell-shape profile of the NO_x emissions in Ontario and Québec, which could
411 be due to either the perturbation from climate anomalies or unrealistic emissions
412 inventory. Considering that the first possibility was minimal over a large regional scale,
413 especially when the consistency was determined in a different time frame (2002-2011)
414 in the same region, it is thus doubtful that the bell-shape profile of the NO_x emissions
415 in 1990-2003 was realistic.

416

417 The regional m-values of NH₄⁺ largely oscillated from 1988 to 2003 (Fig. 5c). The m-
418 values of NH₄⁺, however, decreased by ~30% from 2002 to 2011, leading to a probable
419 decreasing trend in m-value from 1988 to 2011. No correlation was found between the
420 m-values of NH₄⁺ and the emissions of NH₃ in Ontario, which is consistent with the
421 findings at the individual sites discussed above.



422 Since the decrease in F_{wet} values of NO_3^- at Sites 3 and 4 were very likely due to the
423 mitigation of NO_x in Ontario, the decrease also changed the relative contributions
424 between NH_4^+ and NO_3^- in the total N wet deposition budget. For example, NH_4^+ and
425 NO_3^- contributed 52% and 48%, respectively, to the total budget in 2010-2011 and 34%
426 and 66%, respectively, in 1984-1985 at Site 3. The corresponding numbers at Site 4
427 were 58% and 42% in 2010-2011 and 47% and 53% in 1985-1986.

428

429 **4 Conclusions**

430 Climate anomalies during the two-decade period resulted in annual F_{wet} of SO_4^{2-} and/or
431 NO_3^- deviating from the normal value by up to ~40% at the rural Canadian sites. The
432 new approach of rearranging and screening F_{wet} data can largely reduce the impact of
433 climate anomalies when used for generating the decadal trends of F_{wet} . With the climate
434 perturbation being reduced, F_{wet} of SO_4^{2-} exhibited a three-phase decreasing trend at
435 every individual site, as well as on a regional scale in northern Ontario and Québec.
436 The three-phase pattern of the decreasing trend in F_{wet} of SO_4^{2-} matches well with the
437 emission trends of SO_2 in Ontario, as supported by the good correlation between wet
438 deposition and emission, with $r \geq 0.95$ and $P < 0.01$. F_{wet} of NO_3^- exhibited a two-phase
439 decreasing trend, but only during the second phase F_{wet} of NO_3^- , and the emissions of
440 NO_x in Ontario and Québec matched well, with a good correlation of $r \geq 0.91$ and
441 $P < 0.01$. Compared to the results obtained without applying the new approach, it is
442 concluded that, after reducing the perturbation from climate anomalies, 1) better
443 correlation was obtained between F_{wet} of ions and the emission of the corresponding
444 gaseous precursors in northern Ontario and Québec, and 2) the inflection points in the
445 decreasing trends of F_{wet} of SO_4^{2-} and NO_3^- were clearly identified.

446



447 However, the new approach cannot completely remove the perturbations from climate
448 anomalies, especially when this is the dominant factor and/or on long timescales, as
449 was the case at a coastal site of Saturna in British Columbia. At this location, the
450 decreasing trends in F_{wet} of SO_4^{2-} and NO_3^- were caused by the decadal climate
451 anomalies, as well as being affected by interannual climate variability, which
452 overwhelmed the impact of the emission changes of the gaseous precursors in this
453 province. This is the first study that has identified that decadal climate anomalies can
454 dominate trends in F_{wet} of SO_4^{2-} and NO_3^- .

455

456 The long-term variations in F_{wet} of NH_4^+ generally showed no clear long-term trends.
457 Moreover, no apparent cause-effect relationships were found between the wet
458 deposition of NH_4^+ and the emission of NH_3 . This outcome is not surprising because
459 additional key factors besides those discussed in this study also impact the trends of
460 F_{wet} of NH_4^+ . For example, NH_4^+ may be more greatly impacted by changes in SO_2 and
461 NO_x than are NH_3 emissions in NH_3 -rich scenarios. It should be noted that F_{wet} of N
462 via NH_4^+ exceeded those via NO_3^- in 2010 and 2011 in northern Ontario and Québec,
463 where the decrease in F_{wet} of NO_3^- was associated with decreasing NO_x emissions. In
464 contrast, F_{wet} of NH_4^+ did not exceed F_{wet} of NO_3^- in 2010 and 2011 in the coastal area
465 in British Columbia, where the decreasing trends of F_{wet} of NO_3^- were determined to
466 result mainly from the perturbation by climate anomalies.

467

468 *Data availability.* Data used in this study are available from the corresponding authors.

469 *Supplement.* The supplement materials are available online.

470 *Author contribution.* X. Y. and L. Z. designed the study, analyzed the data and prepared the manuscript.

471 *Competing interests.* The authors declare that they have no conflict of interest.

472 *Acknowledgments.* X.Y. is supported by the National Key Research and Development Program in



473 China (No. 2016YFC0200500), and L.Z. by the Air Pollutants program of Environment and Climate
474 Change Canada.

475

476 References

- 477 Baumgardner, R.E., Lavery, T.F., Rogers, C.M., and Isil, S.S.: Estimates of the Atmospheric
478 Deposition of Sulfur and Nitrogen Species: Clean Air Status and Trends Network,
479 1990–2000, *Environ. Sci. & Technol.*, 36, 2614–2629.
480 <https://doi.org/10.1021/es011146g>, 2002.
- 481 Bond, N. A., Overland, J. E., Spillane, M., and Stabeno, P.: Recent shifts in the state of the
482 North Pacific, *Geophys. Res. Lett.*, 30, 2183, <https://doi.org/10.1029/2003GL018597>,
483 2003.
- 484 Burakowski, E. A., Wake, C. P., Braswell, B., and Brown, D. P.: Trends in wintertime climate
485 in the northeastern United States: 1965–2005, *J. Geophys. Res. Atmos.*, 113, 1–12.
486 <https://doi.org/10.1029/2008JD009870>, 2008.
- 487 Butler, T. J., Likens, G. E., Vermeylen, F. M., and Stunder, B. J. B.: The impact of changing
488 nitrogen oxide emissions on wet and dry nitrogen deposition in the northeastern USA,
489 *Atmos. Environ.*, 39, 4851–4862, <https://doi.org/10.1016/j.atmosenv.2005.04.031>, 2005.
- 490 Cheng, I. and Zhang, L. Long-term air concentrations, wet deposition, and scavenging ratios
491 of inorganic ions, HNO₃, and SO₂ and assessment of aerosol and precipitation acidity at
492 Canadian rural locations, *Atmos. Chem Phys.*, 17, 4711–4730,
493 <https://doi.org/10.5194/acp-17-4711-2017>(2017).
- 494 Coopersmith, E. J., Minsker, B. S., and Sivapalan, M.: Patterns of regional hydroclimatic
495 shifts: An analysis of changing hydrologic regimes, *Water Resour. Res.*, 50, 1960–1983.
496 <https://doi.org/10.1002/2012WR013320>, 2014
- 497 Deng, Y., Gao, T., Gao, H., Yao, X., and Xie, L.: Regional precipitation variability in East
498 Asia related to climate and environmental factors during 1979–2012, *Scientific Reports*,
499 4, 5693. <https://doi.org/10.1038/srep05693>, 2014.
- 500 Fagerli, H., and Aas, W.: Trends of nitrogen in air and precipitation: model results and
501 observations at EMEP sites in Europe, 1980–2003, *Environ. Pollut.* 154, 448–461.
502 <https://doi.org/10.1016/j.envpol.2008.01.024>, 2008
- 503 Fowler, D., Smith, R., Muller, J., Cape, J. N., Sutton, M., Erisman, J. W., and Fagerli, H.:
504 Long Term Trends in Sulphur and Nitrogen Deposition in Europe and the Cause of
505 Non-linearities, *Water Air Soil Pollut.*, 7, 41–47. <https://doi.org/10.1007/s11267-006-9102-x>, 2007.
- 507 Fowler, D., Smith, R. I., Muller, J. B. A., Hayman, G., and Vincent, K. J.: Changes in the
508 atmospheric deposition of acidifying compounds in the UK between 1986 and 2001,
509 *Environ. Pollut.*, 137, 15–25, <https://doi.org/10.1016/j.envpol.2004.12.028>, 2005.
- 510 Kampata, J. M., Parida, B. P., and Moalafhi, D. B.: Trend analysis of rainfall in the
511 headstreams of the Zambezi River Basin in Zambia, *Phys. Chem. Earth*, 33, 621–625,
512 <https://doi.org/10.1016/j.pce.2008.06.012>, 2008.
- 513 Pihl Karlsson, G., Akselsson, C., Hellsten, S., and Karlsson, P. E.: Reduced European
514 emissions of S and N – Effects on air concentrations, deposition and soil water
515 chemistry in Swedish forests, *Environ. Pollut.*, 159(12), 3571–
516 3582, <https://doi.org/10.1016/j.envpol.2011.08.007>, 2011.
- 517 Lajtha, K., and Jones, J.: Trends in cation, nitrogen, sulfate and hydrogen ion concentrations



- 518 in precipitation in the United States and Europe from 1978 to 2010: a new look at an old
519 problem, *Biogeochemistry*, 116, 303–334. <https://doi.org/10.1007/s10533-013-9860-2>,
520 2013.
- 521 Lehmann, C. M. B., Bowersox, V. C., Larson, R. S., and Larson, S. M.: Monitoring Long-
522 term Trends in Sulfate and Ammonium in US Precipitation: Results from the National
523 Atmospheric Deposition Program/National Trends Network, *Water Air Soil Pollut.*, 7,
524 59–66. <https://doi.org/10.1007/s11267-006-9100-z>, 2007.
- 525 Li, Y., Schichtel, B. A., Walker, J. T., Schwede, D. B., Chen, X., Lehmann, C. M. B.,
526 Puchalski, M.A., Gay, D.A., and Collett, J. L.: Increasing importance of deposition of
527 reduced nitrogen in the United States, *Proc. Natl. Acad. Sci. U.S.A.*, 113, 5876–5879,
528 <https://doi.org/10.1073/pnas.1525736113>, 2016.
- 529 Lloret, J., and Valiela, I.: Unprecedented decrease in deposition of nitrogen oxides over North
530 America: the relative effects of emission controls and prevailing air-mass trajectories.
531 *Biogeochemistry*, 129, 165–180. <https://doi.org/10.1007/s10533-016-0225-5>, 2016.
- 532 Lynch, J. A., Bowersox, V. C., and Grimm, J. W.: Acid rain reduced in Eastern United States,
533 *Environ. Sci. Technol.*, 34, 940–949. <https://doi.org/10.1021/es9901258>, 2000.
- 534 Marchetto, A., Rogora, M., and Arisci, S.: Trend analysis of atmospheric deposition data: A
535 comparison of statistical approaches, *Atmos. Environ.*, 64, 95–102,
536 <https://doi.org/10.1016/j.atmosenv.2012.08.020>, 2013.
- 537 Monteith, D., Henrys, P., Banin, L., Smith, R., Morecroft, M., Scott, T., Andrew, C.
538 Beaumont, D., Benham, S., Bowmaker, V., Corbet, S., Dick, J., Dod, B., Dodd, N.,
539 McKenna, C., McMillan, S., Pallett, D., Pereira, M.G., Poskitt, J., Rennie, S., Rose,
540 R., Schäfer, S., Sherrin, L., Tang, S., Turner, A., and Watson, H.: Trends and
541 variability in weather and atmospheric deposition at UK Environmental Change
542 Network sites (1993–2012), *Ecol. Indic.*, 68, 21–35.
543 <https://doi.org/10.1016/j.ecolind.2016.01.061>, 2016.
- 544 Rogora, M., Colombo, L., Marchetto, A., Mosello, R., and Steingruber, S.: Temporal and
545 spatial patterns in the chemistry of wet deposition in Southern Alps, *Atmos. Environ.*,
546 146, 44–54. <https://doi.org/10.1016/j.atmosenv.2016.06.025>, 2016.
- 547 Rogora, M., Mosello, R., and Marchetto, A.: Long-term trends in the chemistry of
548 atmospheric deposition in Northwestern Italy: The role of increasing Saharan dust
549 deposition. *Tellus B Chem. Phys. Meteorol.*, 56, 426–434.
550 <https://doi.org/10.1111/j.1600-0889.2004.00114.x>, 2004.
- 551 Sickles II, J. E., and Shadwick, D. S.: Air quality and atmospheric deposition in the eastern
552 US: 20 years of change, *Atmos. Chem. Phys.*, 15, 173–197. <https://doi.org/10.5194/acp-15-173-2015>, 2015.
- 554 Strock, K. E., Nelson, S. J., Kahl, J. S., Saros, J. E., and McDowell, W. H.: Decadal Trends
555 Reveal Recent Acceleration in the Rate of Recovery from Acidification in the
556 Northeastern U.S., *Environ. Sci. Technol.*, 48, 4681–4689.
557 <https://doi.org/10.1021/es404772n>, 2014.
- 558 Teng, X., Hu, Q., Zhang, L.M., Qi, J., Shi, J., Xie, H., Gao, H.W., and Yao, X.H.:
559 Identification of major sources of atmospheric NH₃ in an urban environment in northern
560 China during wintertime, *Environ. Sci. Technol.*, 51, 6839–6848, <https://doi.org/10.1021/acs.est.7b00328>, 2017.
- 562 van Donkelaar, A., R. V. Martin, R. Leaitch, A. M. Macdonald, T. W. Walker, D. Streets, Q.
563 Zhang, E. J. Dunlea, J. Jimenez-Palacios, J. Dibb, L. G. Huey, R. Weber, and M. O.
564 Andreae.: Analysis of aircraft and satellite measurements from the Intercontinental
565 Chemical Transport Experiment (INTEX-B) to quantify long-range transport of East
566 Asian sulfur to Canada, *Atmos. Chem. Phys.*, 8, 2999–3014, <https://doi.org/10.5194/acp-8-2999-2008>, 2008.



- 567 2999-2008, 2008.
- 568 Vet, R., Artz, R. S., Carou, S., Shaw, M., Ro, C.-U., Aas, W., Baker, A., Bowersox, V.C.,
569 Dentener, F., Galy-Lacaux, C., Hou, A., Pienaar, J.J., Gilletti, R., Forti, C., Gromov, S.,
570 Hara, H., Khodzher, T., Mahowald, N.M., Nickovic, S., Rao, P.S.P., and Reid, N. W. A
571 global assessment of precipitation chemistry and deposition of sulfur, nitrogen, sea salt,
572 base cations, organic acids, acidity and pH, and phosphorus, *Atmos. Environ.*, 93, 3–
573 100. <https://doi.org/10.1016/j.atmosenv.2013.10.060>, 2014.
- 574 Vet, R., and Ro, C.-U.: Contribution of Canada–United States transboundary transport to wet
575 deposition of sulphur and nitrogen oxides—A mass balance approach, *Atmos. Environ.*,
576 42, 2518–2529. <https://doi.org/10.1016/j.atmosenv.2007.12.034>, 2008.
- 577 Waldner, P., Marchetto, A., Thimonier, A., Schmitt, M., Rogora, M., Granke, O., Mues, V.,
578 Hansen, K., Pihl Karlsson, G., Zlindra, D., Clarke, N., Verstraeten, A., Lazdins, A.,
579 Schimming, C., Jacoban, C., Lindroos, A.-J., Vanguelova, E., Benham, S., Meesenburg,
580 H., Nicolas, M., Kowalska, A., Apuhtin, V., Napa, U., Lachmanova, Z., Kristoefel, F.,
581 Bleeker, A., Ingerslev, M., Vesterdal, L., Molina, J., Fischer, U., Seidling, W., Jonard,
582 M., O’Dea, P., Johnson, J., Fischer, R., and Lorenz, M.: Detection of temporal trends in
583 atmospheric deposition of inorganic nitrogen and sulphate to forests in Europe, *Atmos.*
584 *Environ.*, 95, 363-37. <http://dx.doi.org/10.1016/j.atmosenv.2014.06.054>, 2014.
- 585 Wetherbee, G. A., and Mast, M. A.: Annual variations in wet-deposition chemistry related to
586 changes in climate, *Clim. Dynam.*, 47, 3141–3155, [https://doi.org/10.1007/s00382-016-](https://doi.org/10.1007/s00382-016-3017-7)
587 3017-7, 2016.
- 588 Wijngaard, J. B., Tank, A. M. G. K., and Können, G. P.: Homogeneity of 20th century
589 European daily temperature and precipitation series. *Int. J. Climatol.*, 23, 679–692,
590 <https://doi.org/10.1002/joc.906>, 2003.
- 591 Wright L.P., Zhang L., Cheng I., Aherne J., and Wentworth G.R.: Impacts and effects
592 indicators of atmospheric deposition of major pollutants to various ecosystems – A
593 review. *Aerosol Air Qual. Res.*, 18, 1953-1992, doi: 10.4209/aaqr.2018.03.0107, 2018
- 594 Wu, Z., and Huang, N. E.: Ensemble empirical mode decomposition: a noise-assisted data
595 analysis method. *Advances in Adaptive Data Analysis*, 1, 1–41,
596 <https://doi.org/10.1142/S1793536909000047>, 2009
- 597 Vieth, E.: Fitting piecewise linear regression functions to biological responses, *J. Appl.*
598 *Physiol.*, 67, 390–396, doi:10.1152/jappl.1989.67.1.390, 1989.
- 599 Yao, X. H., and Zhang, L. Supermicron modes of ammonium ions related to fog in rural
600 atmosphere, *Atmos. Chem. Phys.*, 12, 11165–11178, [https://doi.org/10.5194/acp-12-](https://doi.org/10.5194/acp-12-11165-2012)
601 11165-2012, 2012
- 602 Yao, X., and Zhang, L. Trends in atmospheric ammonia at urban, rural, and remote sites
603 across North America, *Atmos. Chem. Phys.*, 16, 11465–11475,
604 <https://doi.org/10.5194/acp-16-11465-2016>, 2016.
- 605 Zbieranowski, A.L. and Aherne, J.: Long-term trends in atmospheric reactive nitrogen across
606 Canada: 1988–2007, *Atmos. Environ.*, 45, 5853-5862,
607 <https://doi.org/10.1016/j.atmosenv.2011.06.080>, 2011.
- 608 Zhang, L., Jacob, D. J., Knipping, E. M., Kumar, N., Munger, J. W., Carouge, C. C., van
609 Donkelaar, A., Wang, Y.X., and Chen, D.: Nitrogen deposition to the United States:
610 Distribution, sources, and processes, *Atmos. Chem. Phys.*, 12, 4539–4554,
611 <https://doi.org/10.5194/acp-12-4539-2012>, 2012.
- 612 Zhang, L., Vet, R., Wiebe, A., and Mihele, C.: Characterization of the size-segregated water-
613 soluble inorganic ions at eight Canadian rural sites, *Atmos. Chem. Phys.*, 8, 7133–7151,
614 <https://doi.org/10.5194/acp-8-7133-2008>, 2008.



List of Figures

Figure 1. Fitting monthly F_{wet} of SO_4^{2-} against the climatology values from every two years using LR with zero interception at Site 1, according to the new approach described in Section 2. * reflects the maximum value excluded for LR analysis. Fitted lines represent the LR function with zero interception.

Figure 2. m-values and annual F_{wet} extracted trends at Site 1, and the annual emissions of air pollutants in Québec and Ontario, Canada. Full and empty markers in blue in (a), (b) and (g) represent the calculation of m-values without and with the outlier, respectively. Empty markers in red represent the outliers in m-values and are excluded for trend analysis, as detailed in Section 2. R^2 reflects the coefficient of determination of a variable against the calendar year from LR analysis, and the fitted lines represent the LR function.

Figure 3. Identical to Fig. 1, except for Site 2, and the annual precipitation and annual emissions in British Columbia, Canada. Horizontal dashes in (b) represent precipitation, and the fitted lines represent the LR function.

Figure 4. Average wind fields in 1990-2011 (a) and anomalies at 925 hpa in 1990-2001 (b), 2002-2011 (excluding 2007) (c), and 2007 (d) in western coastal Canada and the U.S.

Figure 5. Regional m-values at Sites 1, 3 and 4: (a): SO_4^{2-} , (b): NO_3^- , and (c): NH_4^+ .

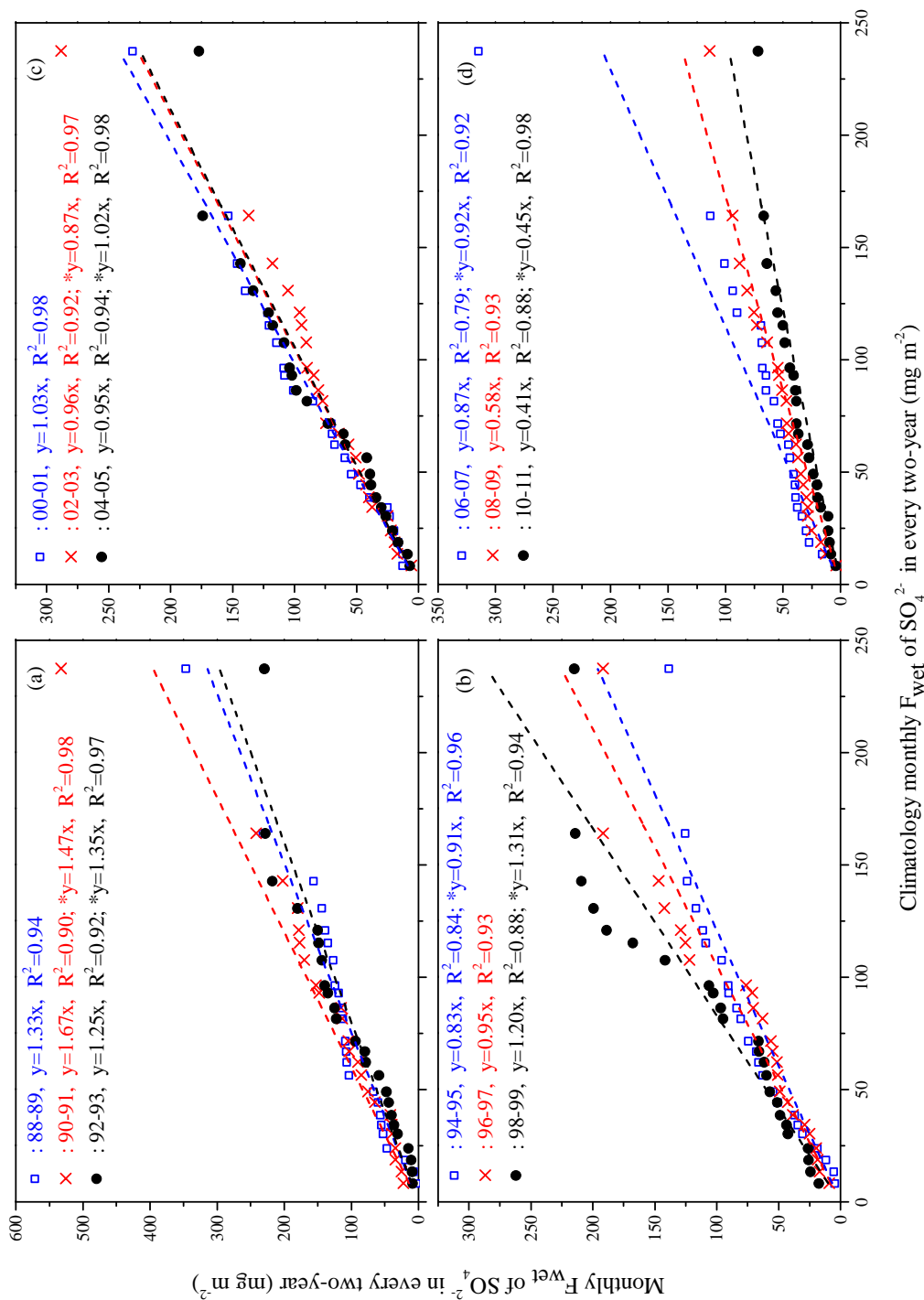


Figure 1. Fitting monthly $F_{\text{wet}}^{\text{SO}_4}$ against the climatology values from every two years using LR with zero interception at Site 1, according to the new approach described in Section 2. * reflects the maximum value excluded for LR analysis. Fitted lines represent the LR function with zero interception.

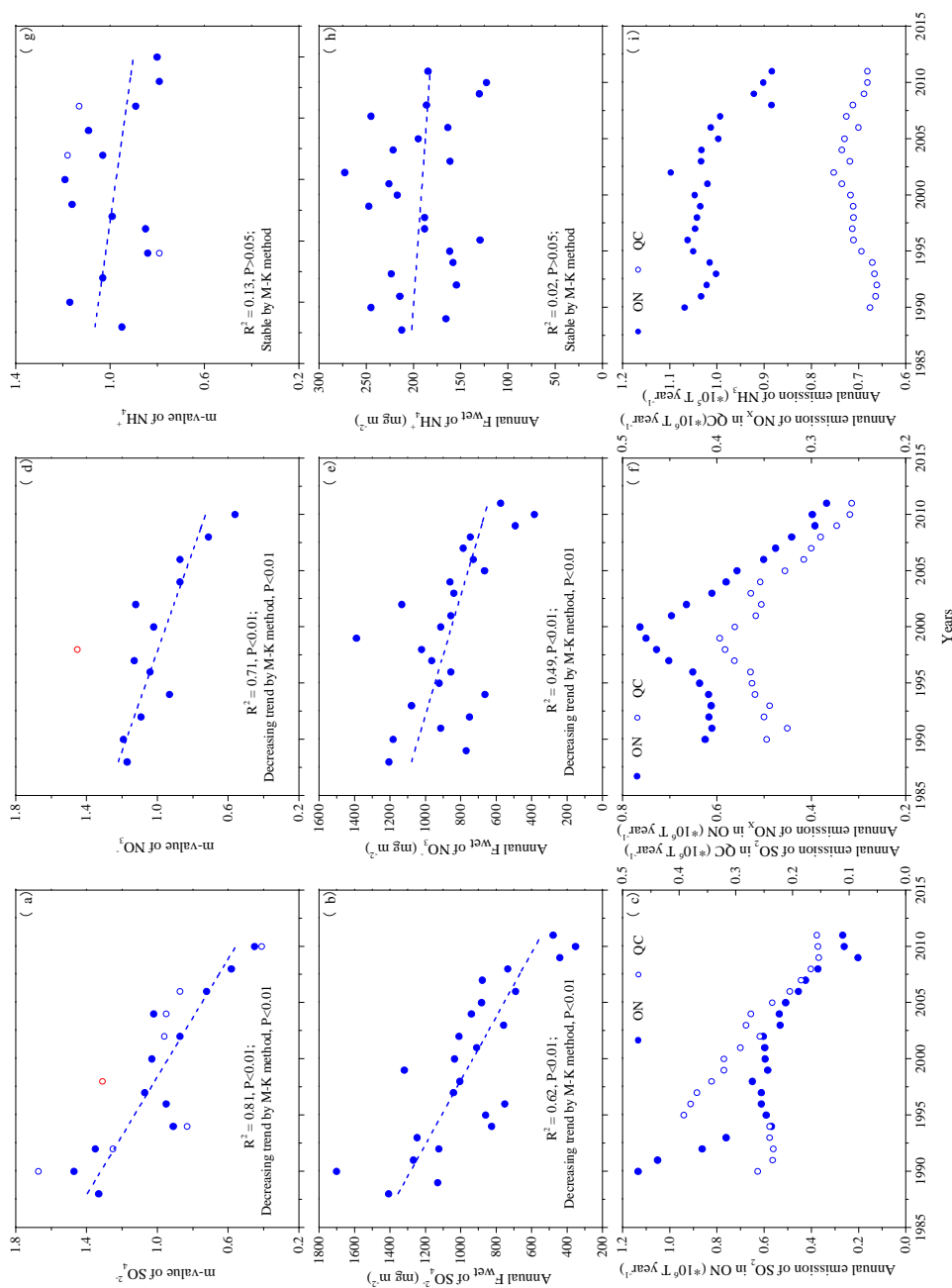


Figure 2. m-values and annual F_{wet} extracted trends at Site 1, and the annual emissions of air pollutants in Québec and Ontario, Canada. Full and empty markers in blue in (a), (b) and (g) represent the calculation of m-values without and with the outlier, respectively. Empty markers in red represent the outliers in m-values and are excluded for trend analysis, as detailed in Section 2. R^2 reflects the coefficient of determination of a variable against the calendar year from LR analysis, and the fitted lines represent the LR function.

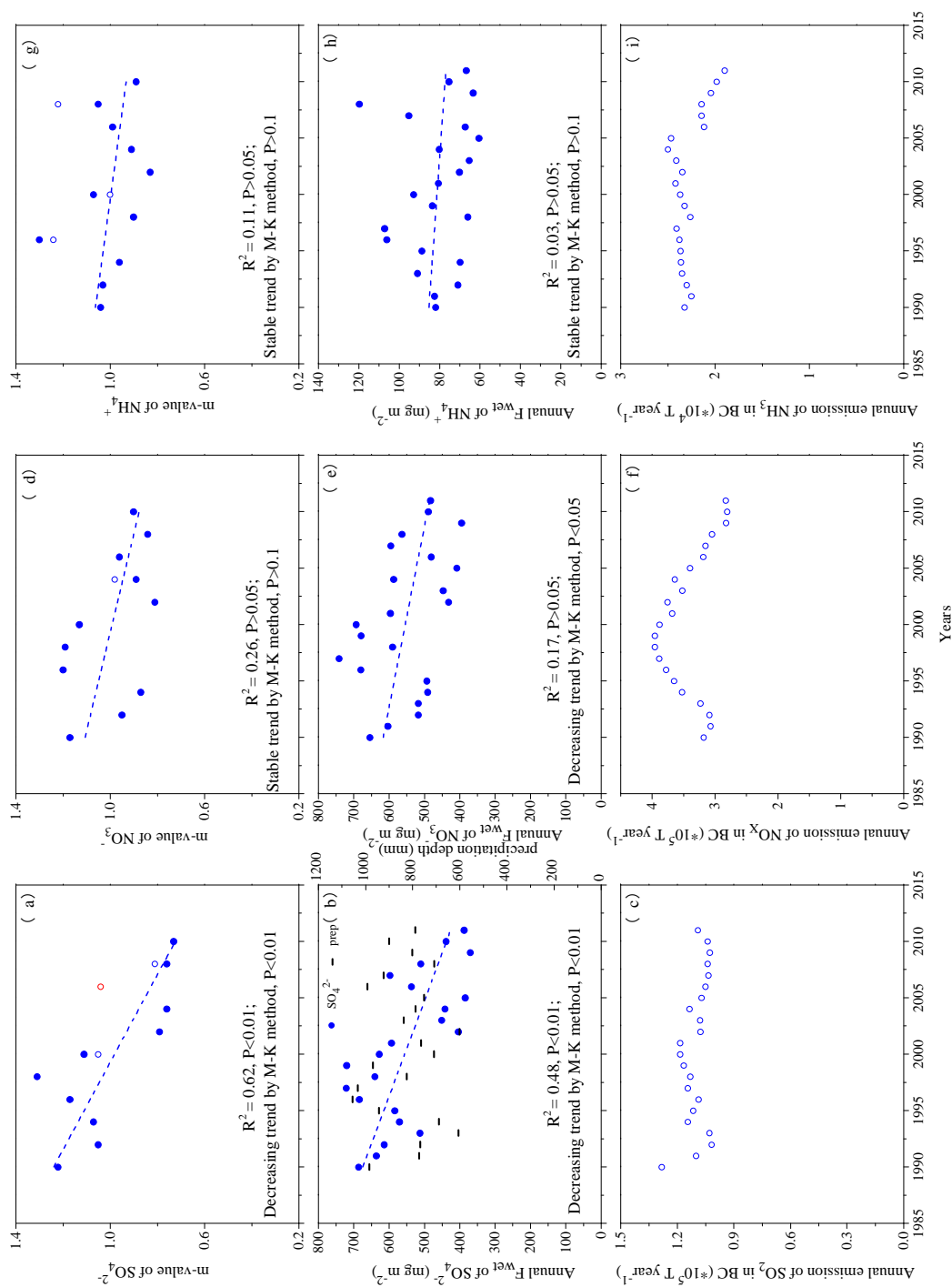


Figure 3. Identical to Fig. 1, except for Site 2, and the annual precipitation and annual emissions in British Columbia,

Canada. Horizontal dashes in (b) represent precipitation, and the fitted lines represent the LR function.

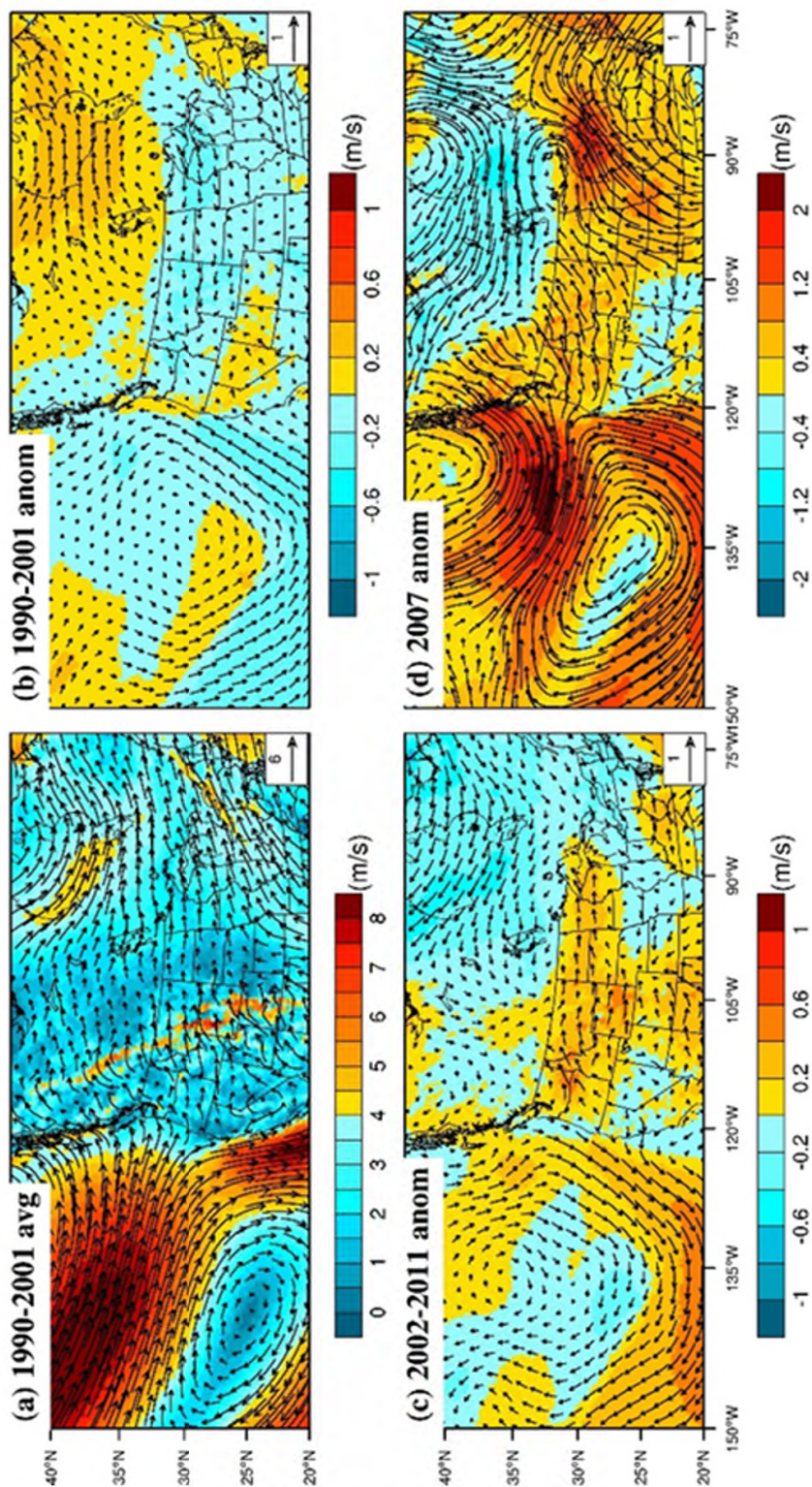


Figure 4. Average wind fields in 1990-2011 (a) and anomalies at 925 hpa in 1990-2001 (b), 2002-2011 (excluding 2007) (c), and 2007 (d) in western coastal Canada and the U.S.

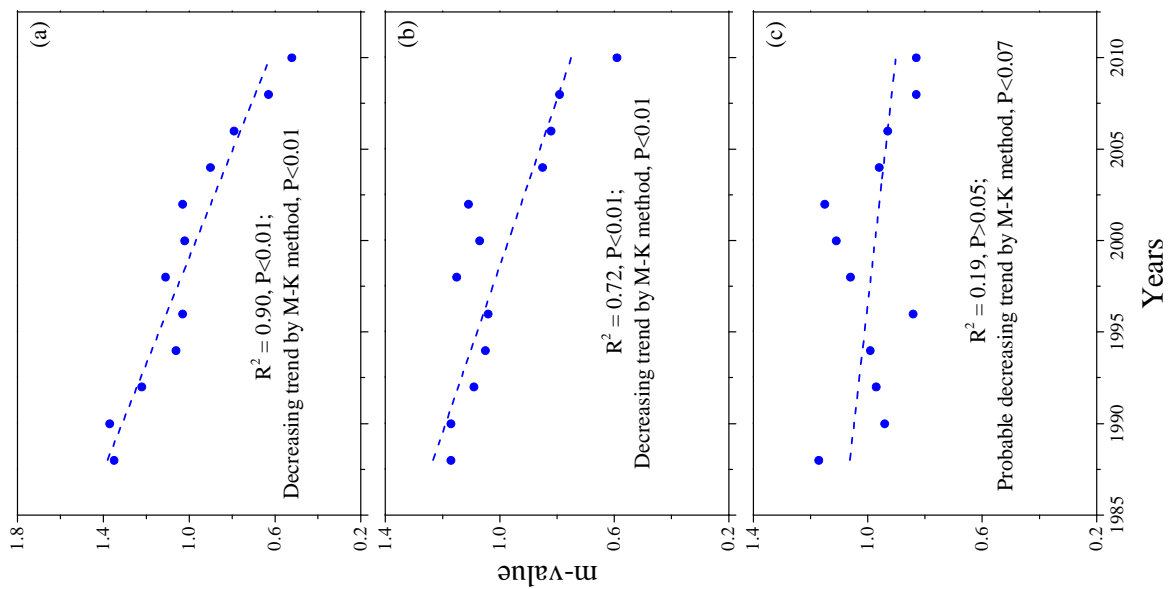


Figure 5. Regional m-values at Sites 1, 3 and 4: (a): SO_4^{2-} ; (b): NO_3^- ; and (c): NH_4^+ .